


Article

Constitutive Material Model for the Compressive Behaviour of Engineered Bamboo

Janeshka Goonewardena , Mahmud Ashraf * , Johannes Reiner, Bidur Kafle  and Mahbube Subhani 

School of Engineering, Faculty of Science, Engineering and Built Environment, Deakin University, Geelong, VIC 3216, Australia

* Correspondence: mahmud.ashraf@deakin.edu.au

Abstract: The mechanical properties of the structural components (i.e., columns and beams produced from engineered bamboo products), such as, bamboo scrimber (also known as parallel bamboo strand lumber, PBSL) and Laminated Bamboo Lumber (LBL), have attracted considerable attention from researchers in recent years. In previous studies, researchers reported on the stress-strain behaviour of bamboo scrimber, LBL and glue laminated bamboo under compression and proposed some empirical and semi-empirical models, based on their individual studies. However, a generic constitutive model for engineered bamboo products is still not available. The compressive stress-strain curves of bamboo scrimber and LBL are reported to show a similar behaviour with three distinct stages i.e., a linear elastic stage followed by a nonlinear plastic stage and a plateau. As part of the current study, the previously proposed models for bamboo scrimber were carefully studied and all available material test results on engineered bamboo were used to develop a generic constitutive model, based on the Ramberg-Osgood (RO) formulation considering its suitability to capture its material nonlinearity. Based on the test results, it was observed that 1% proof stress can be used in a compound RO model to predict an accurate material response for bamboo scrimber. The proposed modelling technique has also been applied to predict the compressive behaviour of LBL. This paper proposes the RO coefficients for both bamboo scrimber and LBL that can be used to develop accurate nonlinear models for engineered bamboo products.

Keywords: bamboo; bamboo scrimber; engineered bamboo; LBL; material model; PBSL; Ramberg-Osgood



Citation: Goonewardena, J.; Ashraf, M.; Reiner, J.; Kafle, B.; Subhani, M. Constitutive Material Model for the Compressive Behaviour of Engineered Bamboo. *Buildings* **2022**, *12*, 1490. <https://doi.org/10.3390/buildings12091490>

Academic Editor: Sardar Malek

Received: 24 August 2022

Accepted: 15 September 2022

Published: 19 September 2022

Publisher's Note: MDPI stays neutral with regard to jurisdictional claims in published maps and institutional affiliations.



Copyright: © 2022 by the authors. Licensee MDPI, Basel, Switzerland. This article is an open access article distributed under the terms and conditions of the Creative Commons Attribution (CC BY) license (<https://creativecommons.org/licenses/by/4.0/>).

1. Introduction

Bamboo is a natural bio composite material that has been used for centuries in various types of structural and non-structural applications, particularly in developing nations [1]. It is the fastest growing plant in the world with a growth rate of 80–300 mm per day [2,3]. Bamboo reaches its maximum height within 4–6 months and matures to its maximum strength within 2–6 years [4], which is significantly less than timber. Bamboo is reported to offer excellent mechanical properties that can be utilised in structural applications [5–8]. Furthermore, bamboo can absorb high levels of CO₂ from the atmosphere during its growth stage [9] and hence, bamboo is often considered as a sustainable, environmentally friendly alternative to traditional construction materials. However, the use of natural bamboo, in major construction, is limited due to size constraints as well as the natural variations in material properties across its thickness and along its length [10].

To overcome these limitations, raw bamboo has been engineered using reasonably consistent manufacturing techniques to produce engineered bamboo products, such as bamboo scrimber and LBL. However, it is worth noting that there are many variants [11–15] to the manufacturing technique of LBL, although the key process of laminating planed rectangular bamboo splits with adhesives remain consistent. Unlike LBL, which can produce considerable post-manufactured bamboo waste, bamboo scrimber utilises 80%

of the raw inputs [16]. Bamboo scrimber consists of crushed bamboo fibre bundles which are saturated in resin and dried into a dense rectangular block under strict moisture conditions. The production process consists of stages of truncating/splitting the bamboo culms, removing the outer layers, defibring, drying, dipping in phenolic resin and finally hot or cold-pressing to form the final bamboo scrimber blocks [17]. It has been noted that bamboo scrimber production requires significantly higher volume of resins and is considerably denser than LBL.

A significant number of studies have recently been reported on the mechanical properties of bamboo scrimber and LBL, subjected to different types of loading. A considerable number of studies focused on concentrically loaded columns made from varying species of bamboo. Sulastiningsih and Nurwati [13] conducted bending and compression tests on laminated bamboo boards made from two species and varying numbers of laminated layers. Li et al. [18] investigated the effect of bamboo growth height on the compressive strength (among other mechanical properties) of laminated bamboo and concluded that the strength increases with the growth height. While Li et al. [19] investigated the effect of length on the crushing of bamboo scrimber columns, Zhao and Zhang [20] extended the investigation by studying the effect of the width on the compression of such columns. Both studies concluded that the design strengths of bamboo scrimber are influenced by length and size effects. Sharma and Gato [21] investigated the effect of the processing methods on the mechanical properties of bamboo and later attributed the difference in the results to the fraction of vascular bundles [22] in the LBL laminates, as bamboo is a functionally graded material. Since bamboo is highly anisotropic, Qiu et al. [23] investigated the mechanical properties of bamboo scrimber with varying fibre orientations and concluded that the classical strength failure criteria, such as the Norris criterion [24] and the Hill-Tsai theory [25], may be used to predict the failure strengths. Moreover, studies were conducted on bamboo scrimber under quasi-static loading [26] and drop-weight penetration impact [27]; the obtained results concluded that the compressive response of bamboo scrimber is strain-rate sensitive and the failure mechanism under drop-weight penetration is highly affected by the fibre orientation. Research on eccentrically compressed columns have also been reported [28–31]. Considering the buckling response, Tan et al. [32,33] and Li et al. [34] conducted compressive tests on intermediate-slender columns made from bamboo scrimber and LBL, respectively. Both concluded that Euler's theorem is only appropriate for long columns while the inelastic buckling theories suit intermediate columns.

In recent years, several studies focused on understanding the compressive properties of engineered bamboo products; however, there is still no widely accepted standard for their structural design. ISO recently developed a design standard for full culm bamboo [35] but this does not provide a platform from which engineers and architects can design engineered bamboo structures [36]. The structural response of engineered bamboo is considerably different from full culm bamboo, and hence, an accurate understanding of the uniaxial behaviour of engineered bamboo is fundamental to the development of any design rule. Similar to its bio composite counterpart timber, the mechanical response of bamboo is highly dependent on fibre orientation; uniaxial resistances are much higher along the fibre direction. Nevertheless, unlike timber, bamboo is significantly stronger in tension, making its behaviour under compression more critical in design.

This paper presents an investigation on the compression behaviour of two commonly used engineered bamboo products i.e., bamboo scrimber and LBL under compression, along the fibre. All existing experimental and analytical work on bamboo scrimber's compression response are thoroughly reviewed to critically evaluate the relevant material models, which were based on a specific set of test results. In this study, all reported test results on the compression response of bamboo scrimber parallel to the fibre direction is analysed, and a modified RO [37] model to capture the material nonlinearity of bamboo is proposed. The concept is also expanded for LBL, and it is found to be in good agreement with the available test results. The proposed RO concept can be used in deriving an analytical formula for bending where material nonlinearity can have a significant effect, as well as in

finite element modelling to accurately predict the structural response of engineered bamboo under various types of loading. A generic constitutive model for engineered bamboo will pave the way for developing reliable and robust structural design rules in order to promote wider usage of bamboo products as an alternative environmentally friendly construction material.

2. Stress-Strain Behaviour of Bamboo and Engineered Bamboo

2.1. Natural Full Culm Bamboo

A unique anatomical feature of bamboo is the embedment of Vascular Bundles (VBs) in a gel-like matrix called parenchyma which provides ductility to bamboo. These VBs also contain the sclerenchyma fibres of bamboo that are responsible for strength and stiffness properties [38,39]. Zhang et al. [40] investigated the compressive behaviour of four and a half year old *Phyllostachys pubescens* highlighting the effect of the VB volume fraction (V_f) on the material behaviour, as shown in Figure 1a, where specimens a-f were extracted from different locations of the culm wall containing 15%, 17%, 22%, 24%, 37% and 46% V_f , respectively. The overall compressive behaviour of bamboo may be divided into three distinct phases before failure—initially a linear elastic response, followed by a nonlinear stage and concluding with a plateau [40]. With the increasing V_f , the initial stiffness and peak stress showed an obvious increase but at the expense of its ductility (as depicted by the length between the red and green dots). This decrease in ductility can be attributed to the decreasing percentage of the parenchyma matrix with the increasing V_f . Shao and Fang [41] investigated the tensile behaviour of four year old *Phyllostachys pubescens* with a varying V_f . Positive correlations were observed for the initial stiffness and maximum tensile strength with respect to the V_f , as shown in Figure 1b. It is evident that the peak tensile stress is significantly higher than the corresponding compressive stress and stress-strain response under tension is linearly elastic till fracture.

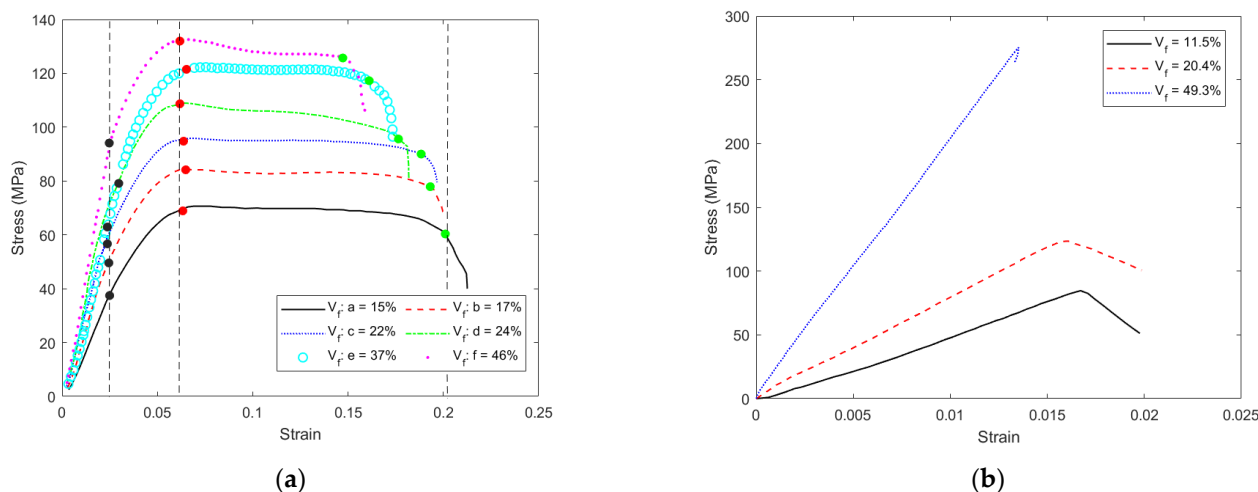


Figure 1. (a) Compressive stress-strain responses of bamboo with varying V_f [40]; (b) Tensile stress-strain response of bamboo with varying V_f [41].

Overall, it is well established, from previous research, that bamboo shows a nonlinear response under compression but produces a linearly elastic response under tension. The tensile strength is significantly higher than the compressive strength, but they are both dependent on the volume fraction of the vascular bundles. Developing a reliable material model for bamboo under compression is, hence, very important for the accurate prediction of the structural response considering the effects of material nonlinearity. Apart from the effects of the VB ratio, research has been conducted on the factors affecting the compressive stress. Li X [42] performed compressive tests on Moso bamboo with a density varying from 490 kg/m^3 to 750 kg/m^3 and observed a doubling of the strength from 47 MPa to 94 MPa, and the modulus of elasticity increased even higher, from 2067 MPa to 4896 MPa. It was

also found that the density increased along the culm from the base to the top. A study [43] was conducted to find the optimum age for the cultivation of bamboo; the trend observed suggests that the mechanical properties were desirable when cultivated between 3–6 years. The moisture content was found to be another contributing factor; a study [44] on *Bambusa pervariabilis* and *Phyllostachys pubescens* showed that the compressive strength less than halved after the fibre saturation point (FSP) whereas the compressive modulus of elasticity remained constant.

2.2. Engineered Bamboo

Engineered bamboo products are manufactured from bamboo culm using various techniques. Tables 1 and 2 show the typical manufacturing variables reported from recent studies on bamboo scrimber and LBL. It is evident that each study consisted of a product that was a function of many variables including bamboo species, age at cultivation, relative growth-height of the bamboo culm (lower, middle and upper), lamination technique (hot or cold-pressed), thermal treatment i.e., saturated steam technique (SST) or hot dry air technique (HDAT), resin, resin content and final moisture content (MC). For LBL, the strip size used in the lamination is important as the strip cross-section determines the V_f , which affects the mechanical properties, as was shown in Figure 1. Figure 2 shows the influence of the manufacturing variables on the compressive stress-strain behaviour, which are plotted based on experimental results shown in Tables 1 and 2.

Table 1. Manufacturing parameters reported in the bamboo scrimber investigations.

Ref.	Species	Age (Years)	Growth-Height	Laminate Method	Thermal Treatment	Resin	Resin Content (%)	Density (kg/m ³)	Final MC (%)
Li et al. [19]	<i>Phyllostachys pubescens</i>	3–4	Upper	Hot-pressed	SST	PF	-	1250	-
Dongsheng et al. [45]	-	5	Upper	Hot-pressed	-	-	-	-	-
Wei et al. [46]	-	-	-	Cold-pressed /heat curing	-	PF	-	-	-
Sheng et al. [47]	<i>Phyllostachys pubescens</i>	5	-	-	-	-	-	-	-
Li et al. [48]	<i>Phyllostachys pubescens</i>	3–4	-	Hot-pressed	SST	PF	-	1254	8.2

SST—Saturated Steam Technique; MC—Moisture Content; PF—Phenol formaldehyde.

Table 2. Manufacturing parameters reported in the LBL investigations.

Ref.	Species	Age (Years)	Growth-Height	Strip Dimensions (mm)		Resin	Density (kg/m ³)	Final MC (%)
				Width	Thickness			
Li et al. [18]	<i>Phyllostachys pubescens</i>	3–4	Upper	17	4	PF	647	8.3
Li et al. [34]	<i>Phyllostachys pubescens</i>	3–4	Lower	21	8	PF	635	7.6
Chen et al. [49]	<i>Phyllostachys pubescens</i>	4	All three heights	-	-	PF	780	10.6

As engineered bamboo products are produced from full-culm bamboo, the similarities in their stress-strain response under compression behaviour are obvious. The compressive behaviour of bamboo scrimber is also nonlinear and shows a combination of elastic and plastic responses, as the stress increases. It should be noted that the compressive test specimens used in this study were limited to a slenderness ratio of 17 and below, to avoid any buckling to capture the pure material response under compression; 17 is the cut-off slenderness ratio for short columns as recommended by ASTM D198 [50]. The elastic limits for bamboo scrimber, based on experimental investigations reported in [19,45–47], were approximately within 55–60% of the ultimate strength, but Li et al. [48] reported a significantly lower elastic limit, based on their test results. Due to the unavailability of all relevant information in those studies (as shown in Table 1), it was difficult to deduce the reasons behind this anomaly.

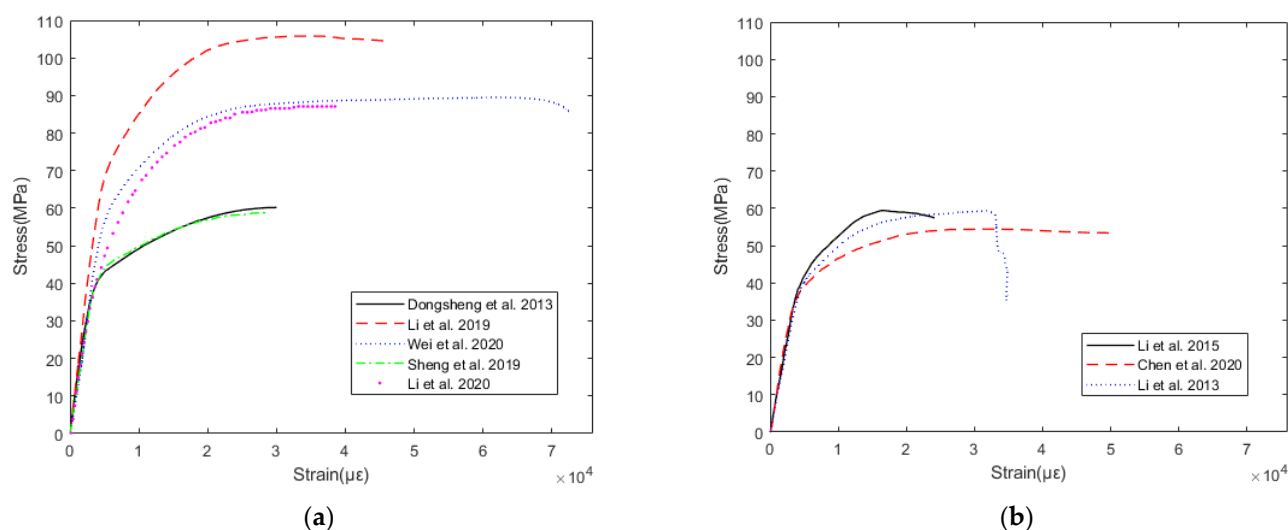


Figure 2. Compressive stress-strain curves for (a) bamboo scrimber [19,45–48]; (b) LBL [18,34,39].

As depicted in Figure 2b, the compressive stress-strain behaviour of LBL is also very similar to bamboo scrimber showing distinct elastic, plastic and plateau stages. However, a few changes can be observed within the elastic and plastic limits, which could be attributed to the differences within the manufacturing processes of LBL (Table 2). Changes in the manufacturing process, such as the layering of multiple lamellae and using strips from different growth heights, are plausible factors for the notable difference. It is worth noting that the tensile stress-strain behaviour of engineered bamboo is similar to raw bamboo and remains linearly elastic till fracture [48,49], and hence is not considered in the current modelling concept.

Despite having some obvious differences in stress and strain values, Figure 2 clearly shows that the stress-strain behaviour of both bamboo scrimber and LBL under compression have a similar rounded and nonlinear response, which resembles nonlinear metallic materials such as aluminium and stainless steel. The RO model was originally developed for aluminium [37] and then was successfully used for other nonlinear metallic materials [51]. Most of the previous studies on bamboo scrimber and LBL proposed empirical material models that were valid only for their reported test results without any real attempt to develop a generic constitutive model. The current study will develop a constitutive model for both bamboo scrimber and LBL based on the RO formula utilising all of the available test results on engineered bamboo.

3. Existing Models for the Compression Behaviour of Engineered Bamboo

The empirical models for modelling the axial compressive stress-strain behaviour of bamboo scrimber were reported by several researchers, based on their own set of experimental results [19,45–48]. Most of the proposed models considered the linear behaviour of bamboo scrimber in the elastic region followed by a nonlinear stress-strain relationship in the plastic region. However, different relationships between stress and strain were reported for the plastic deformation region, such as linear, quadratic and, even, cubic. All previously proposed models for bamboo scrimber are discussed herein by classifying those into two categories i.e., empirical, where the mathematical formulas were derived predominantly based on the regression analysis of the test observations and semi-empirical models, in which the material model is derived based on the test observations, but the relevant formula have some physical significance.

3.1. Empirical Models

3.1.1. Linear Model (LM) by Li et al. [48]

This model approximates the experimentally measured nonlinear stress-strain behaviour to a tri-linear relationship. The linear model is simple when compared with other polynomial models, but it significantly underestimates the stresses in the plastic region.

As depicted in Figure 3a, the linear portion of the elastic-plastic stage is governed by the ratio (k) of secant (E_p) and elastic (E_c) moduli.

$$\sigma(\varepsilon) = \begin{cases} E_c \varepsilon & \varepsilon_{cy} \leq \varepsilon \leq 0 \\ f_{c0} \left[1 - a \left(1 - \frac{\varepsilon}{\varepsilon_{c0}} \right) \right] & \varepsilon_{c0} \leq \varepsilon \leq \varepsilon_{cy} \\ f_{c0} & \varepsilon_{cu} \leq \varepsilon \leq \varepsilon_{c0} \end{cases} \quad (1)$$

$$a = \frac{kn - 1}{n - 1} \quad (2a)$$

$$n = \frac{\varepsilon_{cy}}{\varepsilon_{c0}} \quad (2b)$$

$$k = \frac{E_c \varepsilon_{c0}}{f_{c0}} = \frac{E_c}{E_p} \quad (2c)$$

where, ε is the strain, σ is the stress value for the corresponding ε , E_c is the compressive modulus, ε_{cy} is the yield strain, ε_{c0} is the peak strain/beginning of the plastic plateau, ε_{cu} is the end of the plastic plateau and f_{c0} is the corresponding stress for ε_{c0} .

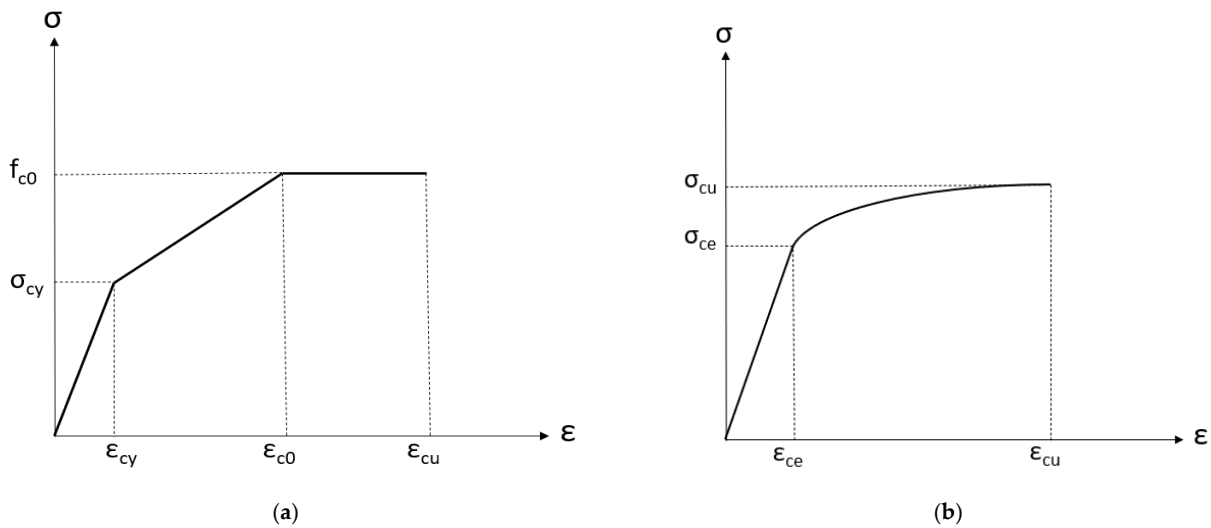


Figure 3. (a) LM (Li et al., 2020) [48]; (b) QM1 by Dongsheng et al., 2013 [45].

3.1.2. Quadratic Model (QM1) by Dongsheng et al. [45]

Dongsheng et al. [45] proposed a quadratic relationship between the stress-strain to capture the nonlinearity observed in their test results. This model is composed of an initial linearly elastic region followed by a quadratic relationship, as shown in Equations (3) and (4). The proposed model uses three coefficients λ_1 , λ_2 and λ_3 , which were determined based on their test results, and the continuum and compatibility conditions of Equation (3).

This model utilises the yield and peak strains, ε_{ce} and ε_{cu} , respectively, as shown in Figure 3b.

$$\sigma(\varepsilon) = \begin{cases} E_c \varepsilon & 0 \leq \varepsilon \leq \varepsilon_{ce} \\ \lambda_1 \varepsilon^2 + \lambda_2 \varepsilon + \lambda_3 & \varepsilon_{ce} \leq \varepsilon \leq \varepsilon_{cu} \end{cases} \quad (3)$$

$$\lambda_1 = -\frac{\sigma_{cu} - \sigma_{ce}}{(\varepsilon_{cu} - \varepsilon_{ce})^2} \quad (4a)$$

$$\lambda_2 = \frac{2\varepsilon_{cu}(\sigma_{cu} - \sigma_{ce})}{(\varepsilon_{cu} - \varepsilon_{ce})^2} \quad (4b)$$

$$\lambda_3 = \frac{\varepsilon_{ce}^2 \sigma_{cu} - 2\varepsilon_{ce} \varepsilon_{cu} \sigma_{cu} + \varepsilon_{cu}^2 \sigma_{ce}}{(\varepsilon_{cu} - \varepsilon_{ce})^2} \quad (4c)$$

where, ε_{cu} is the ultimate compressive strain, ε_{ce} is the strain corresponding to the proportional limit, σ_{cu} is the ultimate compressive stress and σ_{ce} is the yield stress.

Sheng et al. [47] also proposed a quadratic model based on the experimental results of their study on bamboo scrimber. Their approach is very similar to that proposed by Dongsheng et al. [45] and the nonlinear behaviour of the post-elastic stage was simulated by a quadratic polynomial, as shown in Equation (5). The proposed coefficients a_1 , a_2 and a_3 , were calibrated to maintain continuity and compatibility between the linear and nonlinear regions, as shown in Equation (6a–c).

$$\sigma(\varepsilon) = \begin{cases} E_c \varepsilon & | 0 \leq \varepsilon \leq \varepsilon_{ce} \\ a_1(\varepsilon + a_2)^2 + a_3 & | \varepsilon_{ce} \leq \varepsilon \leq \varepsilon_{cu} \end{cases} \quad (5)$$

$$a_1 = -\frac{\sigma_{cu} - \sigma_{ce}}{(\varepsilon_{cu} - \varepsilon_{ce})^2} \quad (6a)$$

$$a_2 = -\varepsilon_{cu} \quad (6b)$$

$$a_3 = \frac{\varepsilon_{ce}^2 \sigma_{cu} - 2\varepsilon_{ce} \varepsilon_{cu} \sigma_{cu} + \varepsilon_{cu}^2 \sigma_{ce}}{(\varepsilon_{cu} - \varepsilon_{ce})^2} \quad (6c)$$

It is, however, worth noting that in their original publication, Sheng et al. [47] made a mistake for coefficient a_3 , which has been rectified herein; Equation (6c) shows the amended expression for a_3 . This amendment made their proposal to be the same as the quadratic model proposed by Dongsheng et al. [45]. Henceforth, both models will be treated as one and will be referred as QM1 for the remainder of this study. Although the quadratic model was shown to replicate the material nonlinearity well, the use of coefficients that do not have any physical significance does not warrant scientific merit. This technique is merely a curve fitting practice, which will require the calibration for each set of experimental data and hence, cannot be accepted as a reliable scientific material model for engineering application.

3.1.3. Quadratic Model (QM2) by Li et al. [19]

Li et al. [19] proposed a quadratic model that consists of a post peak stress stage followed by a linear horizontal stress-strain response, from the peak stress to the ultimate stress. Figure 2a shows the plastic plateau of the experimental curve. The proposed empirical model has a linear peak stress f_{c0} after the ultimate compressive strain to account for the plateau, as depicted in Figure 4a. The parabolic segment of the model is governed by parameter a , which is a function of the ratio of the elastic and secant moduli, as shown by Equations (7) and (8). This formulation is similar to that of the LM (Section 3.1.1).

$$\sigma(\varepsilon) = \begin{cases} E_c \varepsilon & | 0 \leq \varepsilon \leq \varepsilon_{ce} \\ f_{c0} \left[1 + a \left(1 - \frac{\varepsilon}{\varepsilon_{c0}} \right)^2 \right] & | \varepsilon_{ce} \leq \varepsilon \leq \varepsilon_{c0} \\ f_{c0} & | \varepsilon_{c0} \leq \varepsilon \leq \varepsilon_{cu} \end{cases} \quad (7)$$

$$a = \frac{kn - 1}{(n - 1)^2} \quad (8)$$

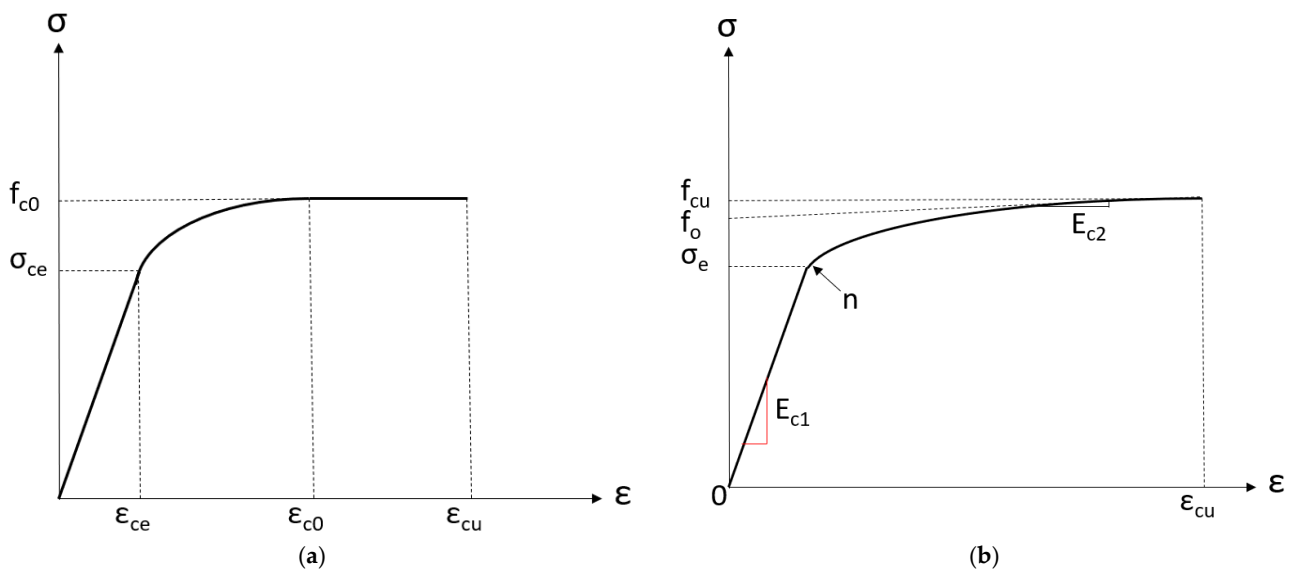


Figure 4. (a) Quadratic Model QM2 by Li et al. (2019, 2020) [19,48]; (b) Richard-Abbott (RA) by Wei et al., 2020 [46].

3.1.4. Cubic Model (CM) by Li et al. [48]

Li et al. [48] also proposed a cubic model for bamboo scrimber made from Moso bamboo with a harvest age of 3–4 years. They used a cubic function of the strain to find the corresponding stress in the elastic-plastic stage, as shown in Equation (9). When this modelling technique was used as part of the current study, the cubic function did not perform well against other test results. It is the authors' view that the cubic model is not a reasonable model to validate with, as a cubic function has two inflection points which is not appropriate for predicting the nonlinear stress-strain response of bamboo/engineered bamboo. This model also gives rise to unnecessary complex formulas, which have very limited practical significance.

$$\Sigma(\epsilon) = \left\{ \begin{array}{l} E_c \epsilon \\ f_{c0} \left[a_0 + a_1 \left(\frac{\epsilon}{\epsilon_{c0}} \right) + a_2 \left(\frac{\epsilon}{\epsilon_{c0}} \right)^2 + a_3 \left(\frac{\epsilon}{\epsilon_{c0}} \right)^3 \right] \\ f_{c0} \end{array} \right\} \begin{array}{l} 0 \leq \epsilon \leq \epsilon_{ce} \\ \epsilon_{ce} \leq \epsilon \leq \epsilon_{c0} \\ \epsilon_{c0} \leq \epsilon \leq \epsilon_{cu} \end{array} \quad (9)$$

$$a_0 = 1 + \frac{2n(kn - 1) + (1 - n)}{(n - 1)^3} \quad (10a)$$

$$a_1 = \frac{2n(3 - 2kn) - k(n + 1)}{(n - 1)^3} \quad (10b)$$

$$a_2 = \frac{(2kn - 3)(n + 1) + 2k}{(n - 1)^3} \quad (10c)$$

$$a_3 = \frac{2 - k(n + 1)}{(n - 1)^3} \quad (10d)$$

3.2. Modified Richard-Abbott (RA) Model by Wei et al. [46]

The RA model [52] is the only constitutive (semi-empirical) model that was used to simulate the stress-strain behaviour of bamboo scrimber in recent studies. The advantage of the RA model over the aforementioned empirical models is its inherent continuity and the use of physical material properties, such as, the compressive moduli and strength instead of empirical constants. Furthermore, it contains a post-elastic compressive modulus (E_{c2})

and a reference plastic stress (f_0) that allow to capture material nonlinearity of engineered bamboo in a rational manner. In the RA model, stress is expressed as a function of strain, as shown in Equation (11).

$$\sigma(\varepsilon) = \left\{ \frac{(E_{c1} - E_{c2})\varepsilon}{\left[1 + \left(\frac{E_{c1} - E_{c2}}{f_0}\varepsilon\right)^n\right]^{\frac{1}{n}}} + E_{c2}\varepsilon \right\} \quad \varepsilon > 0 \quad (11)$$

where, E_{c1} is the initial compressive modulus, f_{cu} is the compressive stress and n is a shape parameter. Wei et al. [46] calibrated this model based on their experimental results obtained from their study. The following values were proposed for bamboo scrimber: $E_{c2} = 0.01E_{c1}$, $f_0 = 0.97f_{cu}$ and $n = 2$; while these values for LBL were reported to be: $E_{c2} = 0.04E_{c1}$, $f_0 = 0.82f_{cu}$ and $n = 2$.

3.3. Limitations of the Existing Models

Most of the existing models are empirically derived and they must be calibrated for coefficients that do not essentially have any physical meaning. The Richard–Abbott model has been shown to perform well for some specific test results. However, the robustness of the proposed models has not been tested as all of the proposed models in literature have been validated using only one dataset.

4. Material Properties of Bamboo Scrimber and LBL under Compression

As shown in Table 1, the current study will utilise all of the available test results on the material properties of both bamboo scrimber and LBL. It is worth noting that all of the data points of the stress-strain plots were not reported in previous studies, and hence, stress-strain data points were extracted using a freely available digital tool WebPlotDigitizer [53]. All of the extracted parameters are listed in Table 3. The listed experimental studies reported multiple curves obtained from several samples, which often showed considerable variations, as expected from a natural biocomposite material such as bamboo. Hence, a representative stress-strain response was selected from the reported data, based on some rational assumptions, as shown in Table 3. The reported deviations in test results are quite natural for bamboo (as well as timber) but the observed discrepancies between the samples did not influence the primary objective of the current study, which is to devise a generic constitutive model that can replicate the overall shape of the stress-strain response of engineered bamboo.

Table 3. Key material parameters extracted from the reported stress-strain behaviour.

Product Type	Experimental Study	E_c (MPa)	ε_{cy} ($\mu\varepsilon$)	ε_{c0} ($\mu\varepsilon$)	f_{cy} (MPa)	f_{c0} (MPa)	Selection Criteria for Representative Stress-Strain Response
Bamboo scrimber	Li et al. [19]	14,275	4380	32,320	62.94	105.79	A sample was chosen with the lowest slenderness ratio which is optimal for failure by compression. This curve pertains to a sample which lies well within the upper and lower curve of all samples examined.
	Dongsheng et al. [45]	11,600	2690	30,010	33.04	60.20	The average curve of the five samples was taken.
	Wei et al. [46]	12,100	4074	61,352	49.71	89.52	The average curve of the compressive samples was taken.
	Sheng et al. [47]	11,440	3060	28,620	35.46	58.81	
	Li et al. [48]	11,320	2900	33,210	33.29	87.08	A stress-strain curve that was well within the upper and lower curves was chosen.
LBL	Li et al. [18]	9200	4220	31,820	36.66	59.36	A sample with the upper growth portion was selected.
	Li et al. [34]	9930	3860	16,760	36.77	59.43	A sample was chosen with the lowest slenderness ratio which is optimal for failure by compression. The source has not specified which test result was taken in the results comparison, however 20 samples were tested.
	Chen et al. [49]	10,880	3140	32,500	32.24	54.48	

E_c —Compressive elastic modulus; ε_{cy} —Compressive yield strain; ε_{c0} —Compressive ultimate strain; f_{cy} —Compressive yield stress; f_{c0} —Compressive ultimate stress.

It should be noted that all of the considered experimental stress-strain curves were taken from stocky columns i.e., columns with a slenderness ratio less than or equal to 17, in order to ensure the observed stress-strain behaviour would represent the material behaviour of bamboo scrimber and LBL.

5. Performance of the Existing Models against All Test Results

Key parameters of the stress-strain models, as presented in Table 3, were used to evaluate the performance of the existing analytical models. As mentioned earlier, each of the existing models were developed based on one study only and hence, their performance against other available results should be evaluated prior to suggesting any modifications. Figure 5 shows the performance of all analytical models for each of the test results reported by researchers to date. The deviations between models and test results are obvious, as expected. Table 4 shows the weighted least squares (WLS) (as shown by Equation (12)) determined for each of the analytical models with respect to the experimental curves.

$$WLS = \frac{1}{n} \sum_{i=1}^n \left| 1 - \frac{\text{theoretical model value}_i}{\text{experimental value}} \right| \quad (12)$$

where, n is the number of points considered in a specific stress-strain plot. It should be noted that the WLS values were calculated up to the peak stress to be consistent as some models do not have guidelines for the post-peak response.

Table 4. WLS values obtained for the existing models against all reported experiments of bamboo scrimber.

Experimental Study	QM 1	QM 2	RA	LM	CM
Li et al. [19]	0.0591	0.0603	0.0697	0.1040	0.1728
Dongsheng et al. [45]	0.0750	0.0698	0.0855	0.1273	0.3211
Wei et al. [46]	0.1093	0.1110	0.0626	0.1669	0.4034
Sheng et al. [47]	0.0389	0.0414	0.0420	0.0976	0.2860
Li et al. [48]	0.0678	0.0700	0.0302	0.1491	0.1397

The WLS method quantifies the absolute variance between two data sets and hence, the lowest WLS value obtained for a model may be considered as an indication of the best possible agreement between the model and considered test results. Table 4 shows the WLS values determined for all of the models and the lowest values for each of the test references is marked in bold to highlight the best fit for each case.

Table 4 shows that both quadratic models QM1 and QM2, which are essentially the same, show good agreement with the experimental stress-strain curves. It is quite evident that while the Richard-Abbott model performed most effectively in two studies, it was also comparable with the quadratic models in the other three studies. The cubic model was poor in comparison with the experimental studies as it significantly overestimates the stress in the plastic region. Even though the linear model was not among the most accurate models, its results are promising, considering its simplicity. The comparisons of each model with the experimental stress-strain curves are shown in Figure 5.

As evident from the WLS values in Table 4 and the plot of the models in Figure 5, the Richard-Abbott model fits closely with two of the experimental studies and has the potential to be modified for further application. E_{c2} , f_0 and n values proposed by Wei et al. [46] show good agreement with other test results reported in [19,45–48], but ideally, further calibrations will be required to apply the RA model for other types of engineered bamboo, based on the species and manufacturing technique and other relevant parameters. Whilst the quadratic and cubic models can be fitted for any test results, the empirical nature of the proposed models is not very scientific as the constants do not have any real physical meaning. The RO model has been widely used in modelling various types of materials as it relies on three easily obtainable parameters. The type of nonlinearity

observed in engineered clearly shows that the RO equation will be a good option for a suitable constitutive model that can have a general applicability for engineered bamboo products. The advantage of the RO equation over the RA model is the usage of a proof strain (p , discussed in the next section) that has the versatility of being changed according to the unique elastic-plastic transitions in biomaterials, such as bamboo. The corresponding proof stress use in the RO formula has been successfully used in designing structural design rules for stainless steel and aluminium, and hence, the same design philosophy could be used for engineered bamboo.

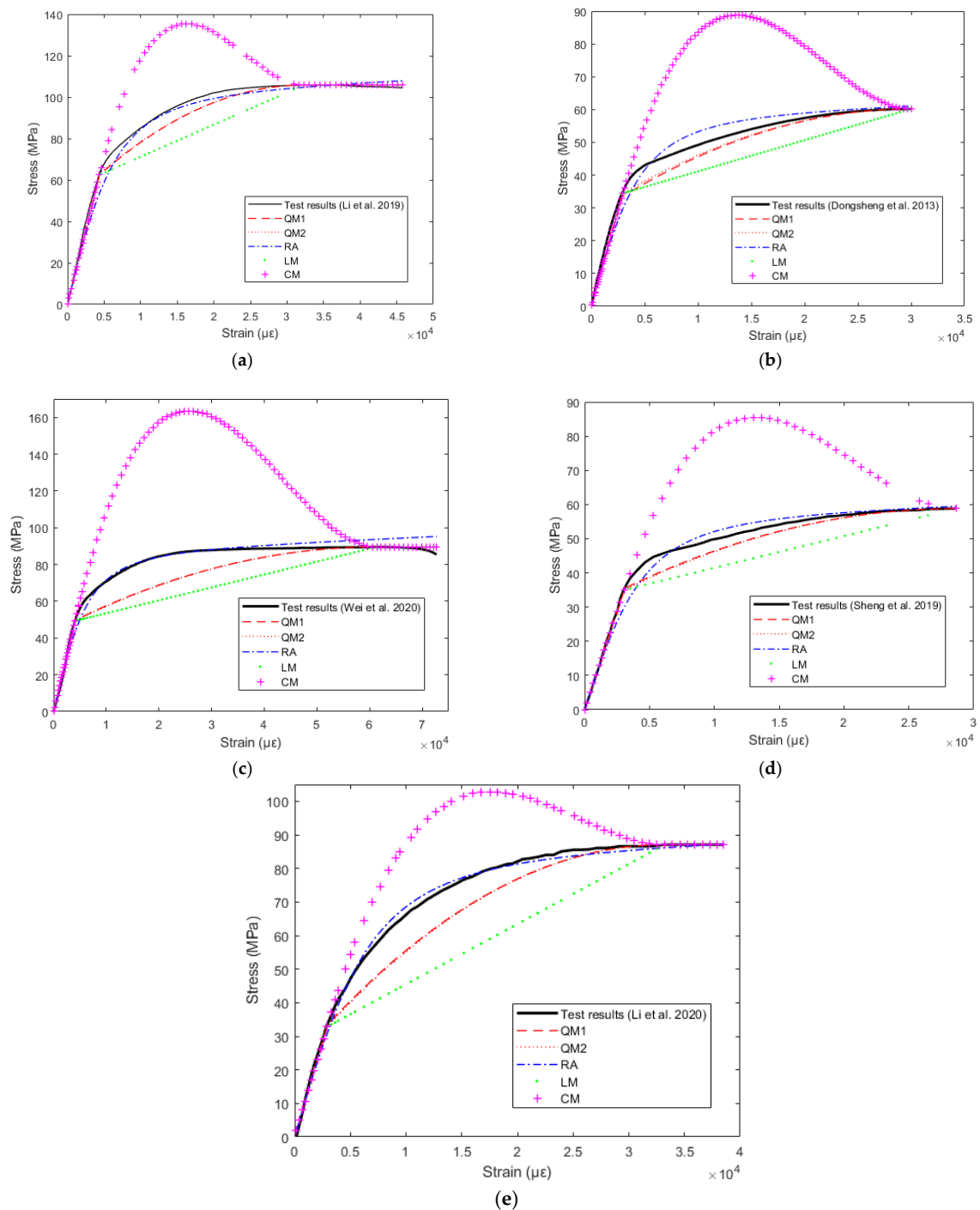


Figure 5. Comparison of the existing models with experimental curves: (a) Li et al., 2019 [19], (b) Dongsheng et al., 2013 [45], (c) Wei et al., 2020 [46], (d) Sheng et al., 2019 [47] and (e) Li et al., 2020 [48].

6. Ramberg-Osgood Model for Engineered Bamboo

6.1. Ramberg-Osgood Material Model [37]

Empirical models, i.e., linear and/or higher order polynomial models proposed in the literature, would typically require the calibration of associated constants against each set of test data to accurately replicate the relevant stress-strain response. The associated constants do not have any physical significance, but their values dictate the shape of the material response. Furthermore, the empirically obtained formulas are not consistent as the post-yield response is different across the experimental studies due to manufacturing variants (Section 2). Analytical models, such as the RA model and the RO model, provide meaningful descriptions of associated key model parameters, which can be obtained from the relevant test data for a specific group of material, as proposed by Ashraf et al. [54] for different stainless-steel grades. In their approach, the RO exponents, which essentially define the accurate shape of the material stress-strain response, were proposed for different material types based on the available test results. In the current study, a similar approach will be adopted to develop the generalised RO models for engineered bamboo products.

The classical RO model, as shown in Equation (13), is also known as the three-parameter model, that requires only three mechanical parameters, i.e., the modulus of elasticity (E_0), the proof stress (σ_p), where p is typically taken as 0.2% (strain) and a dimensionless exponent n , which determines the sharpness of the knee of the stress-strain curve. The proof stress (σ_p) is obtained by offsetting a straight line at the corresponding proof strain (p).

$$\varepsilon = \frac{\sigma}{E_0} + p \left(\frac{\sigma}{\sigma_p} \right)^n \quad (13)$$

Equation (13) was originally calibrated for aluminium, carbon steel and stainless-steel alloys, to simulate their obvious material nonlinearity. A 0.2% proof stress is generally used as the basis for modelling metallic alloys making $p = 0.002$, and hence, Equation (13) takes the well-known form of Equation (14),

$$\varepsilon = \frac{\sigma}{E_0} + 0.002 \left(\frac{\sigma}{\sigma_{0.2}} \right)^n \quad (14)$$

$$n = \frac{\ln 20}{\ln \left(\frac{\sigma_{0.2}}{\sigma_{0.01}} \right)} \quad (15)$$

where, $\sigma_{0.01}$ is the 0.01% proof stress. Figure 6 shows the key parameters in a typical RO simulation for stainless steel alloy.

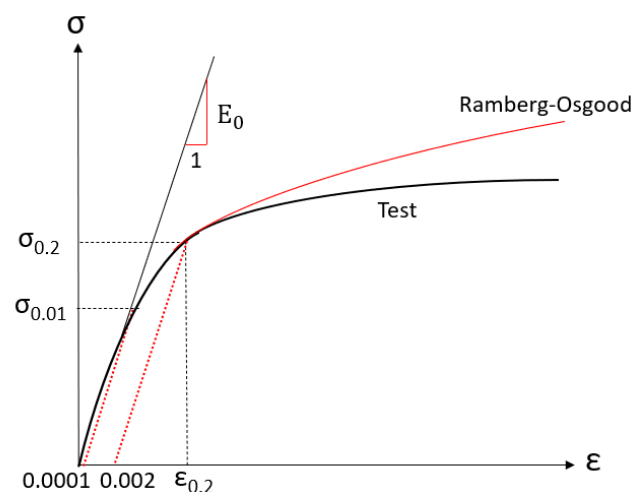


Figure 6. A schematic showing the typical RO stress-strain approximation for stainless steel alloys.

It is worth noting that although the 0.2% proof stress was successfully used for stainless steel alloys, this value can represent any proof stress depending on the stress-strain behaviour of the material under consideration. Although engineered bamboo shows a similar nonlinear response as metals, it is significantly less stiff than metallic alloys. The initial stiffness of engineered bamboo is only 5–8% of steel/stainless steel. As part of the current study, the 0.2%, 0.5% and 1.0% proof stresses were used to find an appropriate proof stress for engineered bamboo based on the considered experimental studies (Table 3). With the introduction of $\sigma_{0.5}$ and $\sigma_{1.0}$, the corresponding RO equations will take the forms, as shown in Equations (16) and (17),

$$\varepsilon = \frac{\sigma}{E_0} + 0.005 \left(\frac{\sigma}{\sigma_{0.5}} \right)^n ; n = \frac{\ln 50}{\ln \left(\frac{\sigma_{0.5}}{\sigma_{0.01}} \right)} \quad (16)$$

$$\varepsilon = \frac{\sigma}{E_0} + 0.01 \left(\frac{\sigma}{\sigma_{1.0}} \right)^n ; n = \frac{\ln 100}{\ln \left(\frac{\sigma_{1.0}}{\sigma_{0.01}} \right)} \quad (17)$$

Figure 7 shows the comparison between the generated RO curves obtained using different proof stresses with the corresponding bamboo scrimber test results reported in the literature. The key parameters, i.e., $\sigma_{0.2}$, $\sigma_{0.5}$, $\sigma_{1.0}$ and n , used in these models were determined from the reported stress-strain response and all of the values are listed in Table 5. It is obvious from Figure 7 that beyond the 0.2% proof stress, the RO curves become inaccurate with the increasing strain in the elastic-plastic region. Use of the 0.5% and 1% proof stresses clearly showed a better performance than the 0.2% proof stress in predicting bamboo scrimber's nonlinear behaviour. Use of the 1.0% proof stress showed an accurate prediction for the nonlinear response, up to the adopted proof stress i.e., $\sigma_{1.0}$. Similar discrepancies i.e., the over or under prediction of stress values, were also significant for both the 0.2% and 0.5% proof stress. This observation clearly shows that the complete stress-strain behaviour may not be accurately predicted by using a single equation. The full-range RO modelling technique has been adopted by several researchers to replicate such behaviour for various nonlinear metallic materials, including high strength steel and stainless steel. It is worth noting that the RO model with a 0.5% proof stress was used by Zhou et al. [55] to compare against the compressive stress-strain behaviour of large-scale bamboo scrimber under local compression. Zhu et al. [56] also proposed the RO model with a 0.3% proof stress for compression parallel to the grain of bamboo scrimber and a 0.1% proof stress for compression transverse to the grain. However, these studies were limited to their own specific test results and did not look at devising any general design guidance for the accurate modelling of engineered bamboo, which is essential for developing reliable numerical models as well as the design rules for engineered bamboo products.

Table 5. Key material properties of bamboo scrimber based on the reported experimental results.

	$\sigma_{0.01}$ (MPa)	$\sigma_{0.2}$ (MPa)	$\sigma_{0.5}$ (MPa)	$\sigma_{1.0}$ (MPa)	e			n			m			E_0 (GPa)	σ_u (MPa)	ε_p
					0.2%	0.5%	1.0%	0.2%	0.5%	1.0%	0.2%	0.5%	1.0%			
Li et al. [19]	49	75	85	97	0.00468	0.00530	0.00605	7.04	7.10	6.74	3.48	3.81	4.21	14.28	105.79	0.03231
Dongsheng et al. [45]	35	43	47.5	53	0.00317	0.00350	0.00390	14.55	12.81	11.10	3.50	3.76	4.08	11.60	60.20	0.03001
Wei et al. [46]	49	63	71	81	0.00492	0.00555	0.00633	11.92	10.55	9.16	3.51	3.82	4.22	12.10	89.52	0.03082
Sheng et al. [47]	37	45.5	49	54	0.00389	0.00420	0.00463	14.49	13.93	12.18	3.71	3.92	4.21	11.44	58.81	0.02862
Li et al. [48]	33	55	68	78.5	0.00453	0.00560	0.00647	5.86	5.41	5.31	3.21	3.73	4.16	11.32	87.08	0.03321

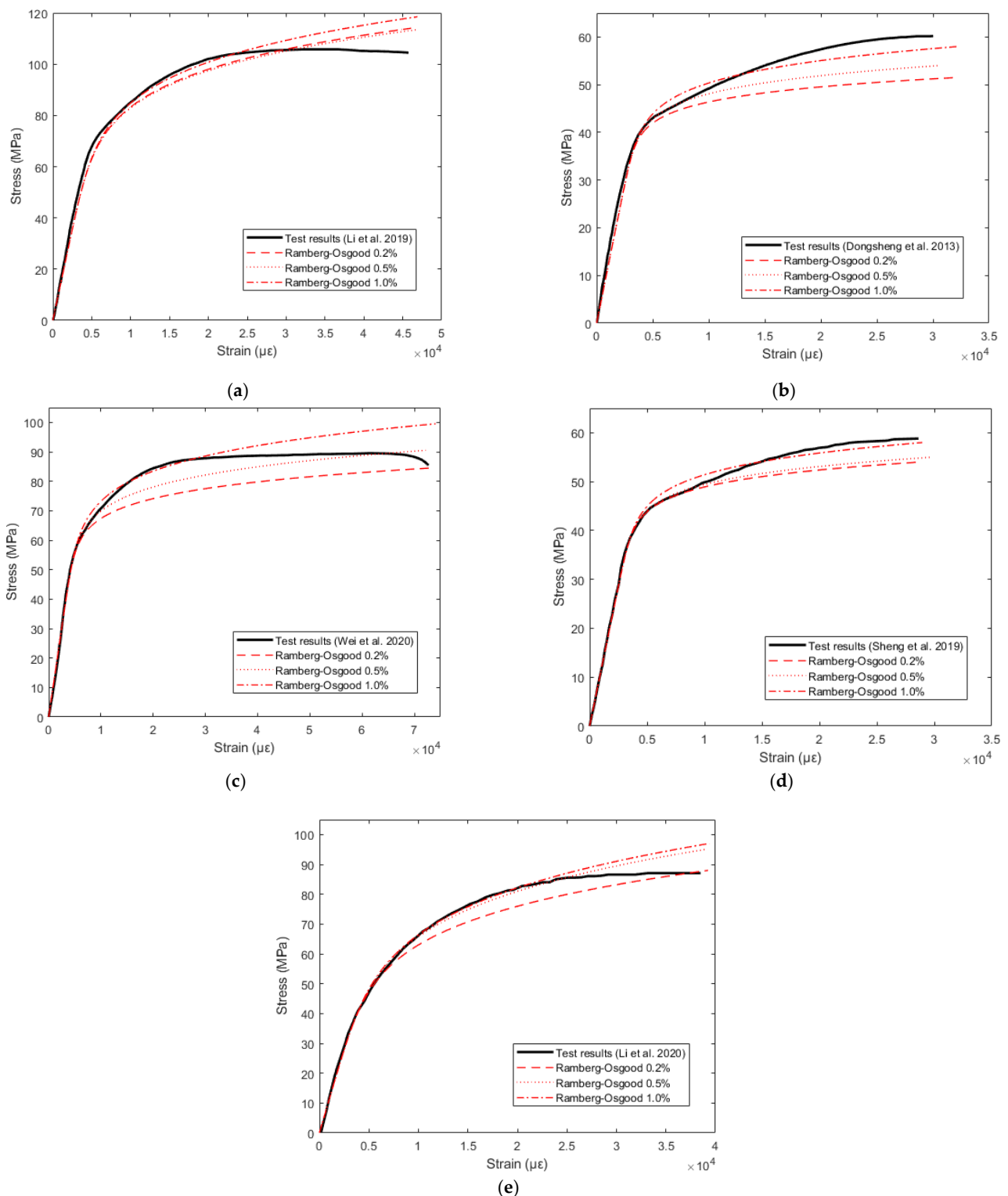


Figure 7. Ramberg-the Osgood approximations using different proof stresses, (a) Li et al., 2019 [19], (b) Dongsheng et al., 2013 [45], (c) Wei et al., 2020 [46], (d) Sheng et al., 2019 [47] and (e) Li et al., 2020 [48].

6.2. Full-Range Ramberg-Osgood Model

Mirambel and Real [57], Ashraf et al. [54] and Rasmussen [58] proposed similar techniques in which a compound RO material model was proposed to simulate the complete nonlinear response demonstrated by stainless steel alloys. In the current study, the full-range RO model proposed by Rasmussen [58] is adopted for its apparent simplicity. The

proposed RO model for bamboo scrimber is divided into two parts: the first part is up to the adopted proof stress $\sigma_{1.0}$, and the second part is from $\sigma_{1.0}$ up to the ultimate stress σ_u . Equation (18) shows the proposed full-range RO model for engineered bamboo.

$$\varepsilon = \begin{cases} \frac{\sigma}{E_0} + 0.01 \left(\frac{\sigma}{\sigma_{1.0}} \right)^n & \left| \sigma \leq \sigma_{1.0} \right. \\ \frac{\sigma - \sigma_{1.0}}{E_{1.0}} + \varepsilon_u \left(\frac{\sigma - \sigma_{1.0}}{\sigma_u - \sigma_{1.0}} \right)^m + \varepsilon_{1.0} & \left. \sigma > \sigma_{1.0} \right\} \quad (18)$$

$$m = 1 + \left(\frac{3.5\sigma_{1.0}}{\sigma_u} \right) \quad (19)$$

$$\varepsilon_{1.0} = e + 0.01 \quad (20)$$

$$E_{1.0} = \frac{E_0}{1 + \frac{0.01n}{e}} \quad (21)$$

$$e = \frac{\sigma_{1.0}}{E_0} \quad (22)$$

where, σ_u is the peak stress, m is an exponent dependent on the peak stress in relation to the proof stress, e is the non-dimensional proof stress and $\varepsilon_{1.0}$ is the corresponding strain at a 1.0% proof stress.

The performance of the full-range RO model and the basic RO model, both with a 1% proof stress, is compared against five representative experimental curves for bamboo scrimber taken from [19,44–47]. Figure 8 shows those comparisons, and it is obvious that the full-range RO model can accurately predict the complete stress-strain response. Values for all of the relevant parameters were determined from the test results and are listed in Table 5.

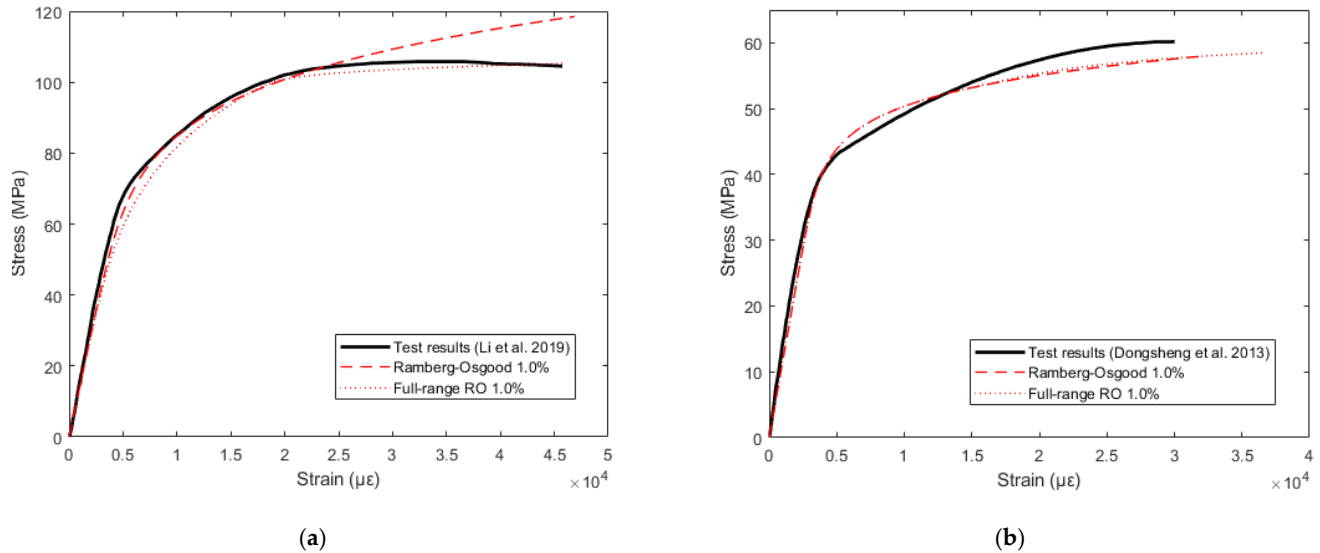


Figure 8. Cont.

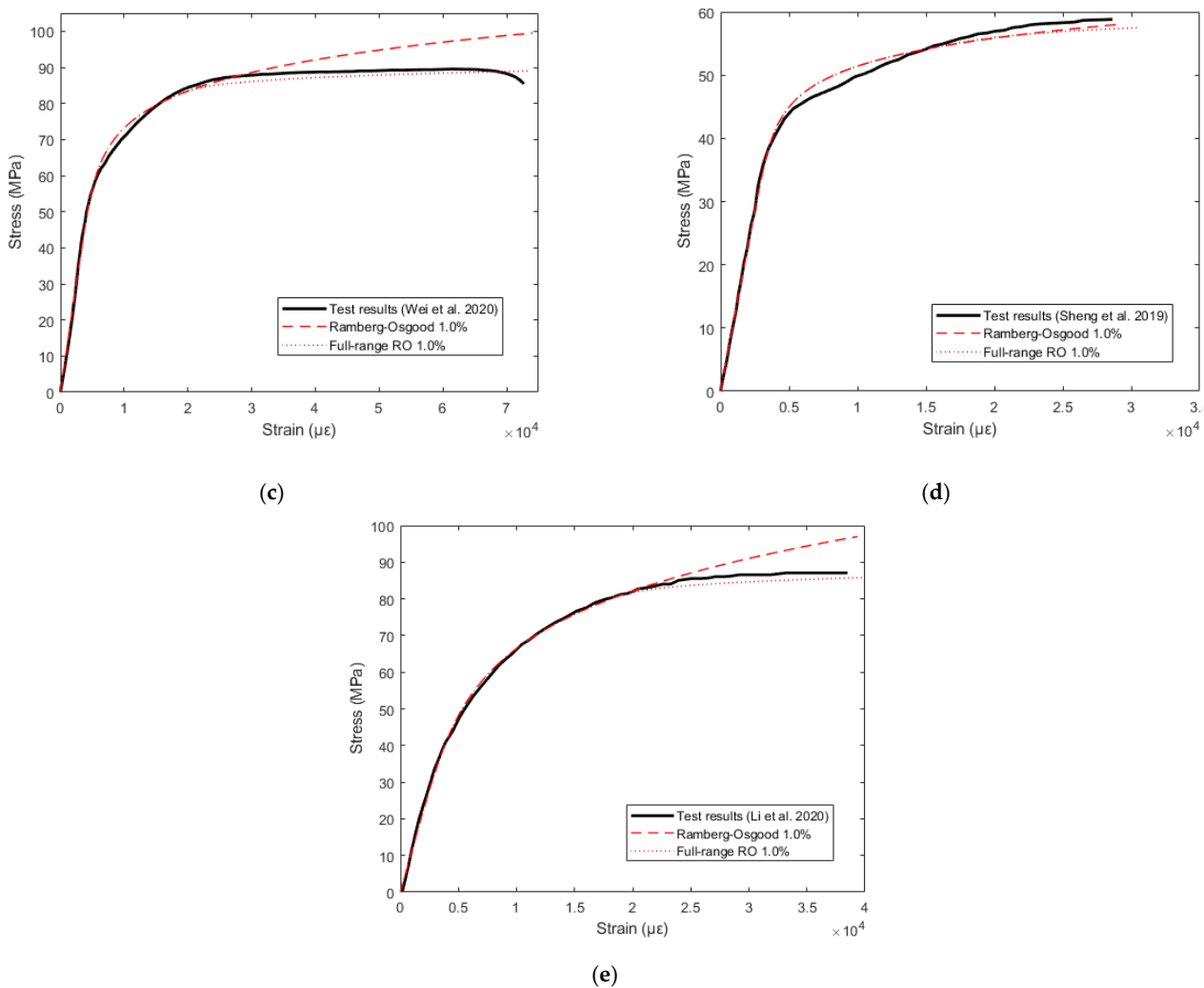


Figure 8. Performance of the full-range RO vs the classical RO with a 1.0% proof stress for bamboo scrimber: (a) Li et al., 2019 [19], (b) Dongsheng et al., 2013 [45], (c) Wei et al., 2020 [46], (d) Sheng et al., 2019 [47] and (e) Li et al., 2020 [48].

6.3. Sensitivity Analysis

A sensitivity analysis was performed for the full-range RO model on the shape parameter (n) for the range $n = 5$ – 13 to find the optimum value to fit all considered experimental curves, which included variations in manufacturing parameters. The experimental curves from studies 1 (19) and 5 (48) have more rounded elastic-plastic transitions. The lower ‘ n ’ values can be attributed to the manufacturing parameters, as both studies have similar properties, as evident from Table 3. This further validates the need for a constitutive model that can capture the inherent material properties of engineered bamboo that can be justified by its manufacturing properties. As the exponent m is within the range of 4.08–4.22, a constant value of $m = 4$ was chosen for the sensitivity analysis. The associated parameters for this sensitivity analysis are shown in Table 5. The effect of the shape factor (n) on the ‘roundedness’ of the curve is shown in Figure 9.

Table 6 shows the weighted least square values for the full-range RO model with varying values of n and the lowest WLS values for each case is highlighted in bold. It is evident that the optimal WLS values were achieved for $n = 7$ – 9 . A comparison is also made with the WLS values for the existing models, and it is evident that the full-range RO model can capture all bamboo scrimber test results quite accurately. With the exception of Li et al. [48], $n = 7$ – 9 produced more accurate curves than the best of the existing models. Therefore, based on the current study and the available test results on bamboo scrimber, the

full range RO model proposed herein (with $n = 7-9$ and $m = 4$) may be used for simulating the structural response.

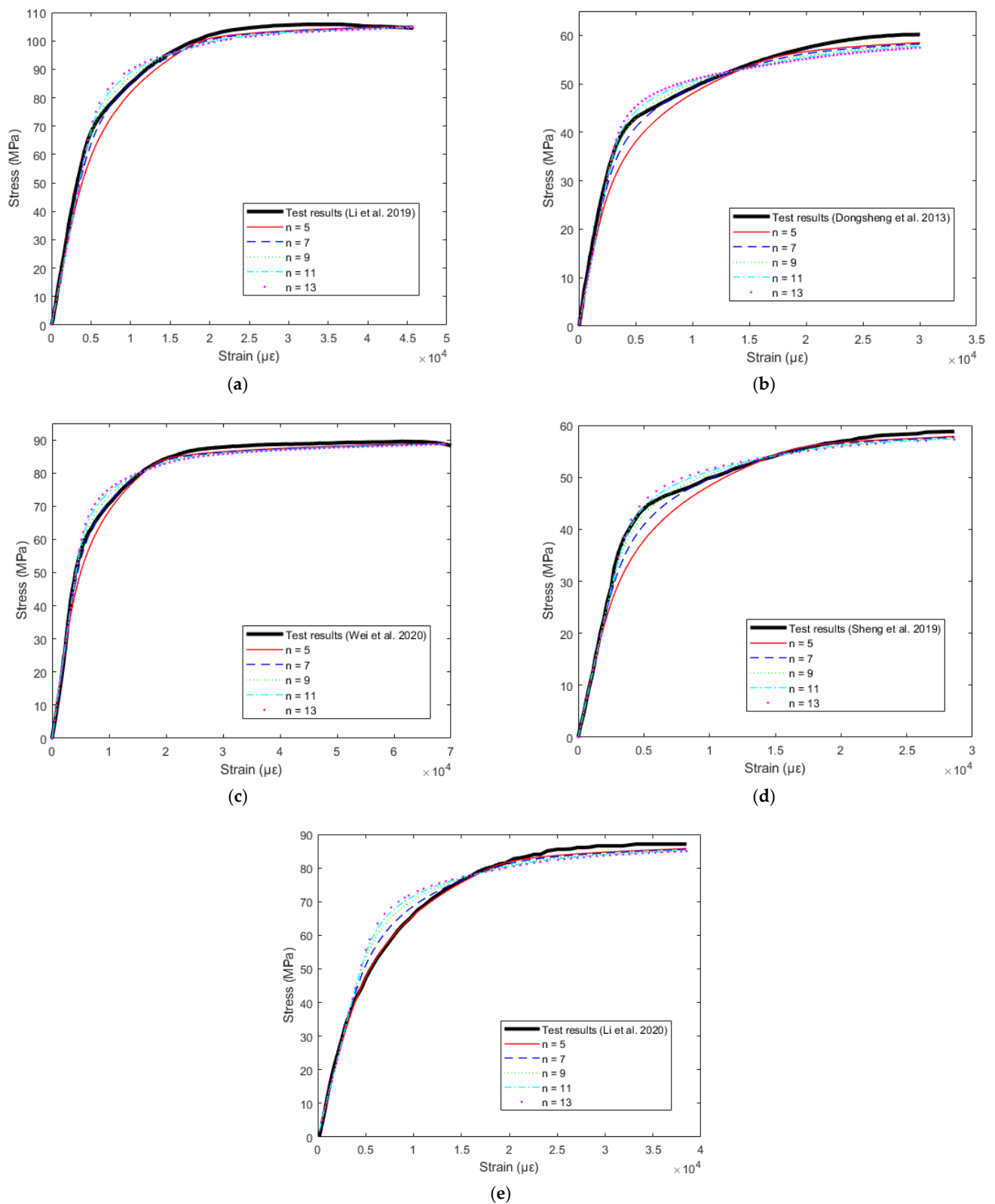


Figure 9. Sensitivity analysis of the shape parameter n for bamboo scrimber experimental studies: (a) Li et al., 2019 [19], (b) Dongsheng et al., 2013 [45], (c) Wei et al., 2020 [46], (d) Sheng et al., 2019 [47] and (e) Li et al., 2020 [48].

Table 6. Weighted least squares of the full-range RO model with $n = 5, 7, 9, 11, 13$.

	'n' for Full-Range RO with 1.0% Proof Stress					Existing Models				
	5	7	9	11	13	QM 1	QM 2	RA	LM	CM
Li et al. [19]	0.0519	0.0385	0.0369	0.0394	0.0420	0.0591	0.0603	0.0697	0.1040	0.1728
Dongsheng et al. [45]	0.0702	0.0531	0.0506	0.0546	0.0604	0.0750	0.0698	0.0855	0.1273	0.3211
Wei et al. [46]	0.0556	0.0459	0.0462	0.0496	0.0529	0.1093	0.1110	0.0626	0.1669	0.4034
Sheng et al. [47]	0.0429	0.0227	0.0175	0.0185	0.0227	0.0389	0.0414	0.0420	0.0976	0.2860
Li et al. [48]	0.0248	0.0353	0.0450	0.0518	0.0570	0.0678	0.0700	0.0302	0.1491	0.1397

7. Proposed Model for Laminated Bamboo Lumber

As the full-range RO model performed satisfactorily for bamboo scrimber, the concept was further extended for LBL. Since the manufacturing process for LBL is different from that of bamboo scrimber, it is imperative to validate the proposed model for LBL. In doing so, it was observed that $n = 7$ and $m = 4$ produced the best fits for the available experimental studies on LBL, as shown in Figure 10. The experimental studies and the material properties for LBL are tabulated in Table 3.

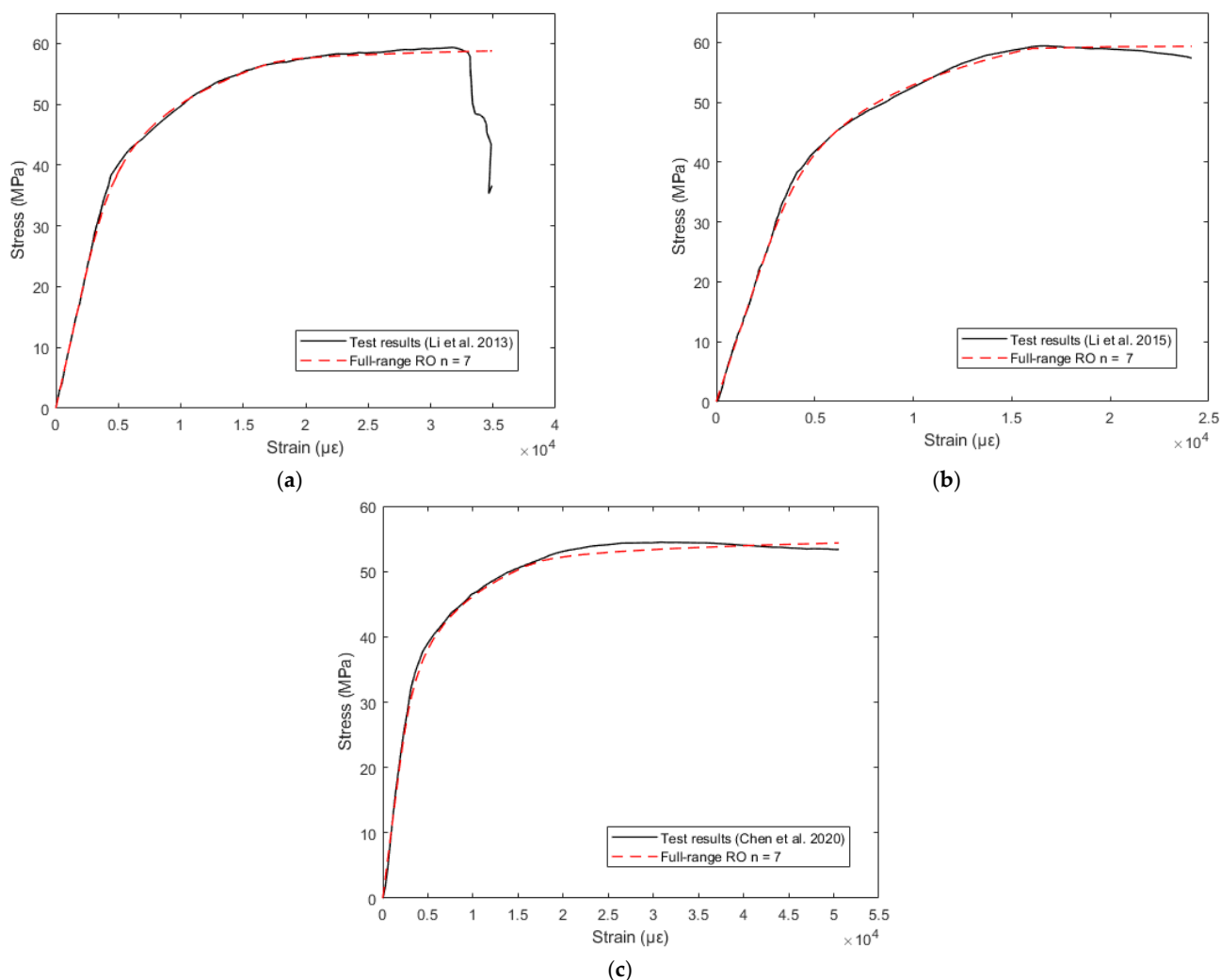


Figure 10. Stress-strain curves for LBL: (a) Li et al., 2013 [18], (b) Li et al., 2015 [34] and (c) Chen et al., 2020 [49].

8. Conclusions

Both bamboo scrimber and LBL manufacturing involves several variables including the bamboo species, adhesives used and a density that can affect the mechanical properties quite significantly. Therefore, each bamboo product has its unique yielding stress and nonlinear elastic-plastic stress-strain response. From the published empirical models in the literature, the quadratic models were shown to be in good agreement with the experimental curves, but those models must be calibrated for associated coefficients that do not often represent any physical significance.

The classical three-parameter Ramberg-Osgood (RO) model was chosen over Richard-Abbott model which requires four parameters for modelling, due to the former's proven suitability in the modelling material nonlinearity for a wide range of materials. It has been shown that the RO can accurately predict the material response of bamboo scrimber up to the 1.0% proof stress, after which it deviates significantly from the experimental curves. To avoid this, the RO equation was split into two parts and the full-range RO model was proposed (Equation (18)). A sensitivity analysis was performed for the shape parameter n and based on the obtained results, $n = 7-9$ and $n = 7$ were proposed for bamboo scrimber and LBL, respectively, while the exponent m is found to be constant and equal to 4. The proposed modelling technique can be easily adopted for any engineered bamboo by knowing the proof stress of the product as the accurate shape of the stress-strain response will be captured by the proposed n and m values. The performance of the proposed full-range RO model has been shown to be significantly better than the previous analytical models proposed for engineered bamboo in the literature. This general material model will be subsequently used for developing rational design rules for compression, bending and the combined actions to promote the use of engineered bamboo in construction.

Author Contributions: Conceptualization, M.A.; data validation, J.G.; investigation, J.G.; writing—original draft preparation, J.G.; writing—review and editing, M.A., M.S., J.R. and B.K.; visualization, M.A., M.S., J.R. and B.K.; supervision, M.A. and M.S. All authors have read and agreed to the published version of the manuscript.

Funding: This research received no external funding.

Institutional Review Board Statement: Not applicable.

Informed Consent Statement: Not applicable.

Conflicts of Interest: The authors declare no conflict of interest.

References

1. Bansal, A.K.; Prasad, T.R.N. Manufacturing laminates from sympodial bamboos—An Indian experience. *J. Bamboo Ratt.* **2004**, *3*, 13–22. [\[CrossRef\]](#)
2. Liese, W. Research on bamboo. *Wood Sci. Technol.* **1987**, *21*, 189–209. [\[CrossRef\]](#)
3. Li, Z.; Liu, C.-P.; Yu, T. Laminate of Reformed Bamboo and Extruded Fiber-Reinforced Cementitious Plate. *J. Mater. Civ. Eng.* **2002**, *14*, 359–365. [\[CrossRef\]](#)
4. Wong, K.M. *The Bamboos of Peninsular Malaysia*; Forest Research Institute Malaysia: Kuala Lumpur, Malaysia, 1995.
5. Awalluddin, D.; Ariffin, M.A.M.; Osman, M.H.; Hussin, M.W.; Ismail, M.A.; Lee, H.-S.; Lim, N.H.A.S. Mechanical properties of different bamboo species. *MATEC Web Conf.* **2017**, *138*, 01024. [\[CrossRef\]](#)
6. Naik, N.K. *Mechanical and Physico-Chemical Properties of Bamboos*; Indian Institute of Technology: Bombay, India, 2009.
7. Molari, L.; Mentrastì, L.; Fabiani, M. Mechanical characterization of five species of Italian bamboo. *Structures* **2020**, *24*, 59–72. [\[CrossRef\]](#)
8. Abdullah, A.; Karlina, N.; Rahmatiya, W.; Mudaim, S.; Fajrin, A. (Eds.) *Physical and Mechanical Properties of Five Indonesian Bamboos*; IOP Conference Series: Earth and Environmental Science; IOP Publishing: Bristol, UK, 2017.
9. Archila-Santos, H.F.; Ansell, M.P.; Walker, P. Low Carbon Construction Using Guadua Bamboo in Colombia. *Key Eng. Mater.* **2012**, *517*, 127–134. [\[CrossRef\]](#)
10. Sharma, B.; Gato, A.; Bock, M.; Mulligan, H.; Ramage, M. Engineered bamboo: State of the art. *Proc. Inst. Civ. Eng.-Constr. Mater.* **2015**, *168*, 57–67. [\[CrossRef\]](#)
11. Andy, W.C.L.; Xuesong, B.; Audimar, P.B. Selected Properties of Laboratory-Made Laminated-Bamboo Lumber. *Holzforschung* **1998**, *52*, 207–210.

12. Nugroho, N.; Ando, N. Development of structural composite products made from bamboo I: Fundamental properties of bamboo zephyr board. *J. Wood Sci.* **2000**, *46*, 68–74. [[CrossRef](#)]
13. Sulastiningsih, I.; Nurwati. Physical and mechanical properties of laminated bamboo board. *J. Trop. For. Sci.* **2009**, *21*, 246–251.
14. Mahdavi, M.; Clouston, P.; Arwade, S. A low-technology approach toward fabrication of Laminated Bamboo Lumber. *Constr. Build. Mater.* **2012**, *29*, 257–262. [[CrossRef](#)]
15. Chen, F.; Jiang, Z.; Deng, J.; Wang, G.; Zhang, D.; Zhao, Q.; Cai, L.; Shi, S.Q. Evaluation of the Uniformity of Density and Mechanical Properties of Bamboo-Bundle Laminated Veneer Lumber (BLVL). *BioResources* **2014**, *9*, 554–565. [[CrossRef](#)]
16. Lugt, P. Design interventions for stimulating bamboo commercialization—Dutch design meets bamboo as a replicable model. Ph.D. Thesis, Delft University of Technology, Delft, The Netherlands, 2008.
17. Huang, Y.; Ji, Y.; Yu, W. Development of bamboo scrimber: A literature review. *J. Wood Sci.* **2019**, *65*, 25. [[CrossRef](#)]
18. Li, H.-T.; Zhang, Q.-S.; Huang, D.-S.; Deeks, A.J. Compressive performance of laminated bamboo. *Compos. Part B Eng.* **2013**, *54*, 319–328. [[CrossRef](#)]
19. Li, H.; Qiu, Z.; Wu, G.; Wei, D.; Lorenzo, R.; Yuan, C.; Zhang, H.; Liu, R. Compression Behaviors of Parallel Bamboo Strand Lumber Under Static Loading. *J. Renew. Mater.* **2019**, *7*, 583–600. [[CrossRef](#)]
20. Zhao, P.; Zhang, X. Size effect of section on ultimate compressive strength parallel to grain of structural bamboo scrimber. *Constr. Build. Mater.* **2019**, *200*, 586–590. [[CrossRef](#)]
21. Sharma, B.; Gatóo, A.; Ramage, M.H. Effect of processing methods on the mechanical properties of engineered bamboo. *Constr. Build. Mater.* **2015**, *83*, 95–101. [[CrossRef](#)]
22. Penellum, M.; Sharma, B.; Shah, D.U.; Foster, R.M.; Ramage, M.H. Relationship of structure and stiffness in laminated bamboo composites. *Constr. Build. Mater.* **2018**, *165*, 241–246. [[CrossRef](#)]
23. Qiu, Z.; Wang, J.; Fan, H.; Li, T. Anisotropic mechanical properties and composite model of parallel bamboo strand lumbers. *Mater. Today Commun.* **2020**, *24*, 101250. [[CrossRef](#)]
24. Norris, C.; McKinnon, P. Compression, Tension, and Shear Tests on Yellow-Poplar Plywood Panels of Sizes that Do Not Buckle with Tests Made at Various Angles to the Face Grain; USDA. 1956. Available online: <https://ir.library.oregonstate.edu/concern/defaults/4q77fw59k> (accessed on 23 August 2022).
25. Tsai, S.W.; Hahn, H.T. *Introduction to Composite Materials*; Routledge: London, UK, 2018.
26. Li, X.; Ashraf, M.; Li, H.; Zheng, X.; Wang, H.; Al-Deen, S.; Hazell, P.J. An experimental investigation on Parallel Bamboo Strand Lumber specimens under quasi static and impact loading. *Constr. Build. Mater.* **2019**, *228*, 116724. [[CrossRef](#)]
27. Li, X.; Ashraf, M.; Li, H.; Zheng, X.; Al-Deen, S.; Wang, H.; Hazell, P.J. Experimental study on the deformation and failure mechanism of parallel bamboo Strand Lumber under drop-weight penetration impact. *Constr. Build. Mater.* **2020**, *242*, 118135. [[CrossRef](#)]
28. Li, H.; Su, J.; Xiong, Z.; Ashraf, M.; Corbi, I.; Corbi, O. Evaluation on the ultimate bearing capacity for laminated bamboo lumber columns under eccentric compression. *Structures* **2020**, *28*, 1572–1579. [[CrossRef](#)]
29. Li, H.-T.; Chen, G.; Zhang, Q.; Ashraf, M.; Xu, B.; Li, Y. Mechanical properties of laminated bamboo lumber column under radial eccentric compression. *Constr. Build. Mater.* **2016**, *121*, 644–652. [[CrossRef](#)]
30. Li, H.-T.; Wu, G.; Zhang, Q.-S.; Su, J.-W. Mechanical evaluation for laminated bamboo lumber along two eccentric compression di-rections. *J. Wood Sci.* **2016**, *62*, 503–517. [[CrossRef](#)]
31. Su, J.-W.; Deeks, A.; Zhang, Q.-S.; Wei, D.D.; Yuan, C.G. Eccentric Compression Performance of Parallel Bamboo Strand Lumber Columns. *Bioresources* **2015**, *10*, 7065–7080.
32. Tan, C.; Li, H.; Wei, D.; Lorenzo, R.; Yuan, C. Mechanical performance of parallel bamboo strand lumber columns under axial compression: Experimental and numerical investigation. *Constr. Build. Mater.* **2020**, *231*, 117168. [[CrossRef](#)]
33. Tan, C.; Li, H.; Ashraf, M.; Corbi, I.; Corbi, O.; Lorenzo, R. Evaluation of axial capacity of engineered bamboo columns. *J. Build. Eng.* **2021**, *34*, 102039. [[CrossRef](#)]
34. Li, H.-T.; Su, J.-W.; Zhang, Q.-S.; Deeks, A.J.; Hui, D. Mechanical performance of laminated bamboo column under axial compression. *Compos. Part B Eng.* **2015**, *79*, 374–382. [[CrossRef](#)]
35. *IT. ISO 22156; 2021 Bamboo Structures—Bamboo Culms—Structural Design*. BSI Standards Limited: London, UK, 2021.
36. Harries, K.A.; Sharma, B.; Richard, M. Structural Use of Full Culm Bamboo: The Path to Standardization. *Int. J. Arch. Eng. Constr.* **2012**, *1*, 66–75. [[CrossRef](#)]
37. Ramberg, W.; Osgood, W.R. *Description of Stress-Strain Curves by Three Parameters*; NASA Scientific and Technical Information: Washington, DC, USA, 1943.
38. Ochi, S. Mechanical Properties of Uni-Directional Long Bamboo Fiber/Bamboo Powder Composite Materials. *Mater. Sci. Appl.* **2014**, *05*, 1011–1019. [[CrossRef](#)]
39. Xie, J.; Qi, J.; Hu, T.; De Hoop, C.F.; Hse, C.Y.; Shupe, T.F. Effect of fabricated density and bamboo species on physical–mechanical properties of bamboo fiber bundle reinforced composites. *J. Mater. Sci.* **2016**, *51*, 7480–7490. [[CrossRef](#)]
40. Zhang, X.; Li, J.; Yu, Z.; Yu, Y.; Wang, H. Compressive failure mechanism and buckling analysis of the graded hierarchical bamboo structure. *J. Mater. Sci.* **2017**, *52*, 6999–7007. [[CrossRef](#)]
41. Shao, Z.-P.; Fang, C.-H.; Huang, S.-X.; Tian, G.-L. Tensile properties of Moso bamboo (*Phyllostachys pubescens*) and its components with respect to its fiber-reinforced composite structure. *Wood Sci. Technol.* **2010**, *44*, 655–666. [[CrossRef](#)]

42. Li, X. Physical, Chemical, and Mechanical Properties of Bamboo and Its Utilization Potential for Fiberboard Manufacturing. Master's Thesis, Louisiana State University, Baton Rouge, LA, USA, 2004. [[CrossRef](#)]
43. Sanchez, L. *Bamboo as a Sustainable Engineering Material: Mechanical Properties, Safety Factors, and Experimental Testing*; University of South Florida: Tampa, FL, USA, 2019.
44. Chung, K.; Yu, W. Mechanical properties of structural bamboo for bamboo scaffoldings. *Eng. Struct.* **2002**, *24*, 429–442. [[CrossRef](#)]
45. Dongsheng, H.; Aiping, Z.; Yuling, B. Experimental and analytical study on the nonlinear bending of parallel strand bamboo beams. *Constr. Build. Mater.* **2013**, *44*, 585–592. [[CrossRef](#)]
46. Wei, Y.; Zhou, M.; Zhao, K.; Zhao, K.; Li, G. Stress–strain relationship model of glulam bamboo under axial loading. *Adv. Compos. Lett.* **2020**, *29*, 2633366X20958726. [[CrossRef](#)]
47. Sheng, B.; Bian, Y.; Liu, Y.; Chui, Y.-H. Experimental Study of the Uniaxial Stress-strain Relationships of Parallel Strand Bamboo in the Longitudinal Direction. *BioResources* **2019**, *14*, 13.
48. Li, H.; Zhang, H.; Qiu, Z.; Su, J.; Wei, D.; Lorenzo, R.; Yuan, C.; Liu, H.; Zhou, C. Mechanical Properties and Stress Strain Relationship Models for Bamboo Scrimber. *J. Renew. Mater.* **2020**, *8*, 13–27. [[CrossRef](#)]
49. Chen, G.; Yu, Y.; Li, X.; He, B. Mechanical behavior of laminated bamboo lumber for structural application: An experimental investigation. *Eur. J. Wood Wood Prod.* **2020**, *78*, 53–63. [[CrossRef](#)]
50. ASTM International. *Standard Test Methods of Static Tests of Lumber in Structural Sizes*; ASTM DASTM International: West Conshohocken, PA, USA, 2009.
51. Gardner, L.; Ashraf, M. Structural design for non-linear metallic materials. *Eng. Struct.* **2006**, *28*, 926–934. [[CrossRef](#)]
52. Richard, R.M.; Abbott, B.J. Versatile Elastic-Plastic Stress-Strain Formula. *J. Eng. Mech. Div.* **1975**, *101*, 511–515. [[CrossRef](#)]
53. Rohatgi, A. WebPlotDigitizer; Austin, Texas, USA, 2017. Available online: <https://automeris.io/WebPlotDigitizer/> (accessed on 23 August 2022).
54. Ashraf, M.; Gardner, L.; Nethercot, D.A. Structural Stainless Steel Design: Resistance Based on Deformation Capacity. *J. Struct. Eng.* **2008**, *134*, 402–411. [[CrossRef](#)]
55. Zhou, K.; Li, H.; Hong, C.; Ashraf, M.; Sayed, U.; Lorenzo, R.; Corbi, I.; Corbi, O.; Yang, D.; Zuo, Y. Mechanical properties of large-scale parallel bamboo strand lumber under local compression. *Constr. Build. Mater.* **2020**, *271*, 121572. [[CrossRef](#)]
56. Zhu, W.; Qiu, Z.; Zhou, J.; Jin, F.; Fan, H. Size design and nonlinear stress-strain relationship of parallel bamboo strand lumbers in tension and compression. *Eng. Fail. Anal.* **2022**, *140*, 106587. [[CrossRef](#)]
57. Mirambell, E.; Real, E. On the calculation of deflections in structural stainless steel beams: An experimental and numerical investigation. *J. Constr. Steel Res.* **2000**, *54*, 109–133. [[CrossRef](#)]
58. Rasmussen, K.J. Full-range stress–strain curves for stainless steel alloys. *J. Constr. Steel Res.* **2003**, *59*, 47–61. [[CrossRef](#)]